

# Influence of pounding with retaining walls on the response of base-isolated structures, Part 1: Numerical case study

○中澤俊幸<sup>1)</sup>・曲哲<sup>2)</sup>・吉敷祥一<sup>3)</sup>

1) 非会員 東京建築研究所 工修, e-mail: nakazawa-t@tkse2000.co.jp

2) 非会員 東京工業大学 PD 研究員・PhD, e-mail: m.quzhe@gmail.com

3) 正会員 東京工業大学 助教・博士(工学), e-mail: kishiki@serc.titech.ac.jp

## 1. Introduction

Increasing attentions have been devoted to pounding behavior of base-isolated buildings with surrounding retaining walls. Through nonlinear dynamic analysis of a generic base-isolated reinforce concrete (RC) frame, the pounding response and its influence is demonstrated.

## 2. Model description

The generic superstructure is a 3-story RC moment-resisting frame (Figure 1), which is designed in accordance with AIJ recommendation<sup>[1]</sup>. A single bay of the frame is modeled as a plane frame in ABAQUS 6.8 and fiber-based beam element with user-defined materials for the concrete and steel rebar fibers (Figure 2a and 2b) is used to model the RC components. Mass-proportional damping is adopted and 2% damping ratio is assigned for the 1<sup>st</sup> mode of the superstructure.

The base mat of the superstructure is surrounded by elastic-perfectly plastic retaining walls at a clearance of 500mm (Figure 2c). The retaining wall has an initial stiffness  $k_w$  of 12700kN/m, about 10% of the 1<sup>st</sup> story stiffness, and a strength  $F_{wy}$  of 884.2kN that is 20% of the total weight of the superstructure.

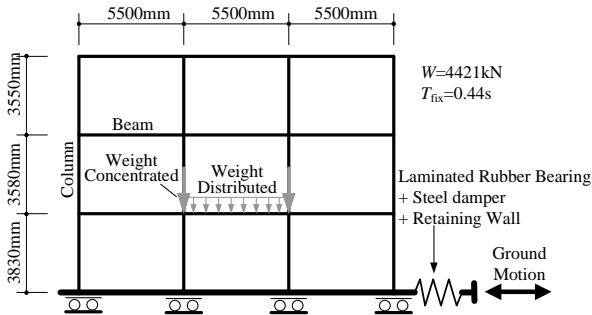


Figure 1 Generic base-isolated frame model

The isolation layer is composed of natural rubber bearings (NRB) and steel dampers. Nonlinear hysteretic model with trilinear skeleton curve and energy dissipation in the hardening regime (Figure 2d) is adopted for NRB, following the proposal of Nakanishi (2007)<sup>[2]</sup>. The initial stiffness of the NRB  $k_{NRB}$  is assumed to be 1100kN/m, leading to an isolation period of 4.0s (i.e. the period of an SDOF system with stiffness  $k=k_{NRB}$ ). Linear elastic limit strain is 250% and the total rubber thickness  $nt_R$  is set to be 200mm. As a result, the linear elastic limit deformation of

NRB is 500mm, the same as the retaining wall clearance. Fracture behavior of NRB beyond 450% strain is not modeled. Instead, very large stiffness is assigned.

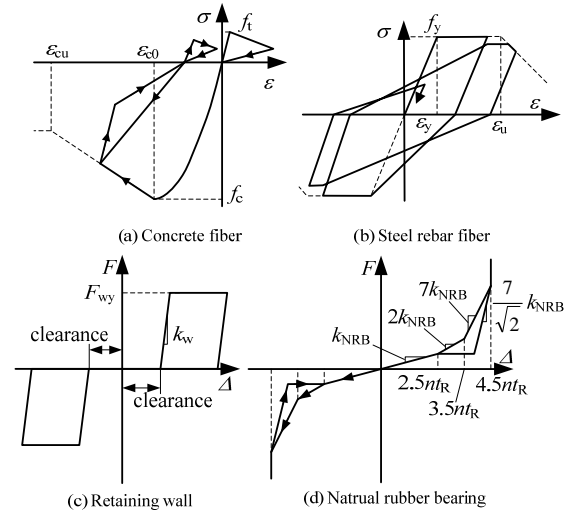


Figure 2 Hysteretic models

## 3. Earthquake ground motion record

The NS component of the record at station CHY101 during the M7.6 Chichi earthquake in 1999 is adopted herein. It is feathered by its high peak ground velocity PGV=114.9cm/s. Its peak ground acceleration PGA is 0.44g.

## 4. Analysis result

The seismic responses of 3 models i.e. (a) Fixed based model; (b) Isolated model and (c) Ideally isolated model are assessed and compared.

In the “Ideally isolated model”, there is no retaining wall and NRB is assumed linear elastic throughout the analysis. The above 3 models are denoted as “Fix”, “Iso” and “Ideal Iso” hereafter.

During the ground motion, the base mat collides with the retaining wall twice at 19.8s and 21.5s, respectively. Figure 3(a) shows the reaction force of the retaining wall due to the impact. In Figure 3(b), the 1<sup>st</sup> floor interstory drift of the “Iso” and “Ideal Iso” models during these poundings are compared. Sudden increase of the interstory drift can be observed during each collision. It is also notable that higher frequency vibration is stimulated by the first collision. The impact velocity can be read from Figure 3(c), which is the relative velocity of the base mat at the

instant of impact. The base mat velocities of the “Iso” and “Ideal Iso” models are identical until the onset of the first collision of the “Iso” model, which alters the base mat velocity time history from the “Ideal Iso” case and has an influence on the impact velocities of consequent collisions.

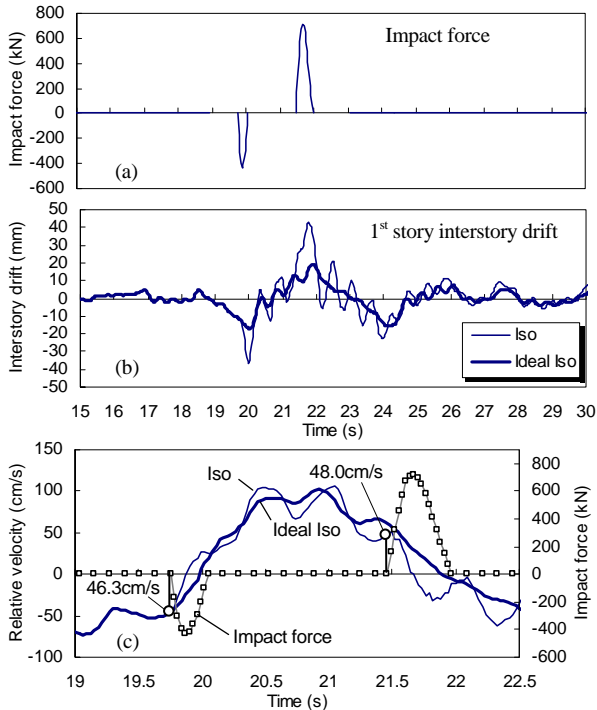


Figure 3 Time history response of isolated models

The increase of deformation is accompanied with sudden changes of inertia forces acting on each story. Figure 4(a) depicts the variation of story shear force during the 1<sup>st</sup> collision. Those of the “Ideal Iso” model are also depicted for comparison. The story shear change is obtained by subtracting the shear forces of the “Ideal Iso” model from those of the “Iso” model.

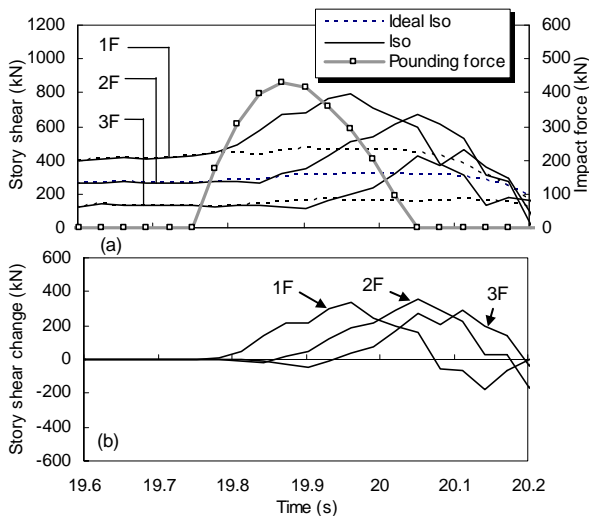


Figure 4 Story shear force during pounding

Before pounding, the two models behave exactly the same. The 1<sup>st</sup> collision with an impact velocity of 46.3cm/s

gives an obvious rise in the shear force of the 1<sup>st</sup> story. This rise then travels along the height of the building to the 2<sup>nd</sup> and the 3<sup>rd</sup> story. The story shear change is depicted in Figure 4b. The travel of the pounding-induced input energy along the height the structure can be clearly seen.

Figure 5 compares the maximum interstory drift ratio and floor acceleration of the 3 models. Ideal isolation can provides superior protection to the superstructure by significantly reducing both the interstory drift and the floor acceleration. However, pounding obviously impairs the advantages of base-isolation. For the current case, the maximum story drift ratio of the “Iso” model is about twice that of the “Ideal Iso” model, although it is still much lower than that of the “Fix” model. Furthermore, the maximum absolute acceleration of the base mat of the “Iso” model is even greater than the peak ground acceleration. It is also obvious from Figure 6 that the damage of the “Iso” model is much more significant than that of the “Ideal Iso” model.

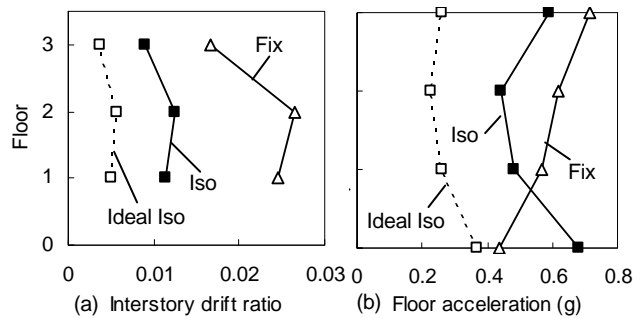


Figure 5 Peak responses of the 3 models

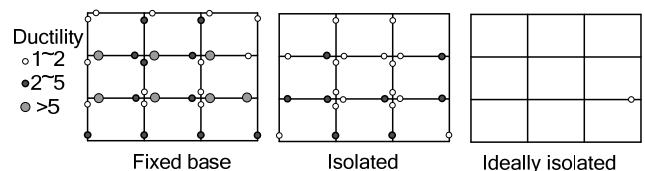


Figure 6 Damage of the superstructures of the 3 models

## 5. Concluding remarks

As revealed by the above analysis results, pounding with the retaining wall is likely to impose a significant lateral action on the superstructure and this action travels along the height of the superstructure. As a result, the deformation and the corresponding damage of not only the first floor of the superstructure, but also the upper floors would be considerably increased in comparison with the ideally isolated case. Furthermore, the floor acceleration of the ground floor can also be greatly increased and may exceed the peak ground acceleration at the bottom floor. This may impose a critical demand for protections of contents in this floor.

Reference  
See Part 2

# Influence of pounding with retaining walls on the response of base-isolated structures, Part 2: Validity of lumped mass MDOF model

○曲哲<sup>1)</sup>・中澤俊幸<sup>2)</sup>・吉敷祥一<sup>3)</sup>

1) 非会員 東京工業大学 PD研究員・PhD, e-mail: m.quzhe@gmail.com

2) 非会員 東京建築研究所 工修, e-mail: nakazawa-t@tkse2000.co.jp

3) 正会員 東京工業大学 助教・博士(工学), e-mail: kishiki@serc.titech.ac.jp

## 1. Introduction

The validity of the commonly-used lumped mass model needs to be carefully examined before extending its application into evaluating the seismic response of base-isolated buildings, especially when pounding needs to be taken into account.

## 2. Lumped mass MDOF model

The superstructure is usually condensed into a lumped mass MDOF model, where the mass of each story is represented by a lumped mass with only one degree of freedom. The restoring force of each story is represented by a horizontal spring. For the RC frame in this study, trilinear hysteresis as shown in Figure 1 is used.

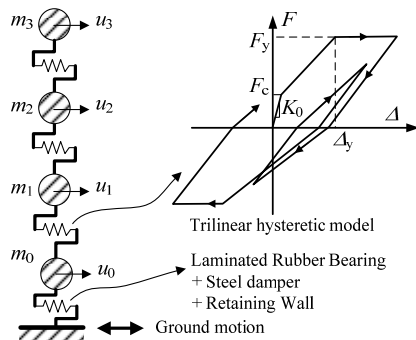


Figure 1 Lumped mass MDOF model

Nonlinear static analysis is carried out to generate “pushover curves” of the frame model. By tri-linearizing the pushover curves, the initial stiffness  $K_0$ , crack strength  $F_c$ , yield strength and deformation  $F_y$  and  $\Delta_y$  can be determined. Another two parameters of the hysteretic model i.e. the post-yield stiffness ratio  $\alpha$  and the unloading stiffness factor  $\beta$  are set as  $\alpha=0.001$  and  $\beta=0.4$ .

Two lateral load distributions are used in the pushover analysis: (1) The modal superposition method in AIJ recommendation for loads<sup>[3]</sup> and (2) The Ai distribution.

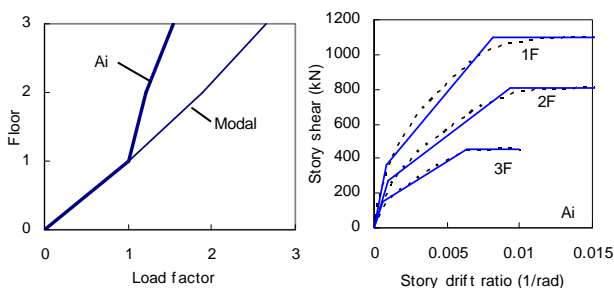


Figure 2 Lateral force distribution and pushover curves

Figure 2 compares the two distributions and depicts the tri-linearization of the pushover curves by the “modal” distribution. Two 3DOF models with different hysteretic parameters can thus be built. They are denoted as “Modal” and “Ai”, respectively.

## 3. Earthquake ground motion record

The NS component of the CHY101 record in the 1999 M7.6 Chichi earthquake and the rotated A-TMZ000 record in the 1976 M6.5 Friuli earthquake are adopted herein. The CHY101-N record is the same as in Part 1. It is not scaled in the following analysis. The A-TMZ000 is scaled to  $PGV=100\text{cm/s}$  for the “Fix” model and  $PGV=350\text{cm/s}$  for the “Iso” and “Ideal Iso” models.

## 4. Analysis result

The seismic responses of 3 structures i.e. (a) Fixed based; (b) Isolated and (c) Ideally isolated structure are assessed and compared. In the “Ideally isolated” structure, there is no retaining wall and the NRB is assumed linear elastic throughout the analysis. The above 3 structures are denoted as “Fix”, “Iso” and “Ideal Iso” hereafter.

Figure 3 compares the maximum interstory drift of the 3 structures subjected to the above mentioned 2 ground motion records. Results estimated by different numerical models, i.e. the member-by-member frame model and the 3DOF “Modal” and “Ai” models are plotted in the same graph.

It is observed from the results of “Fix” and “Iso” structure that accuracy of 3DOF models is strongly dependent on the ground motion record. The pounding may reduce this dependency by imposing a significant pulse action to the structure. As observed for the “Iso” structure, both the 3DOF models tend to concentrate most the deformation in the 1<sup>st</sup> floor, which is not the case for the member-by-member frame model. By examining the time history responses, it is found that the two models experienced different collisions (Figure 4a). The impact velocity at the major collision of the 3DOF (Modal) model is as high as  $84.6\text{cm/s}$ , which is about 1.8 times the pounding velocity of the frame model. This will lead to excessive deformation of the 3DOF model.

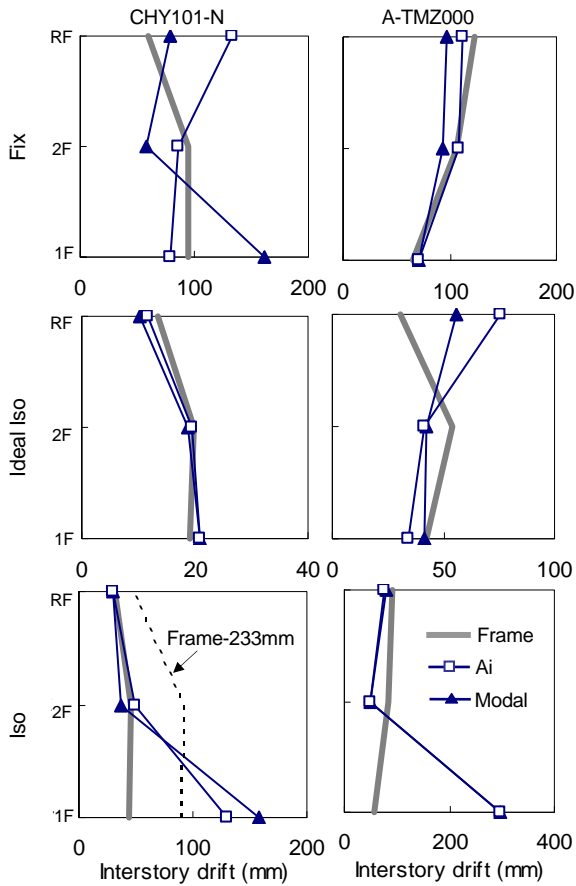


Figure 3 Maximum interstory drift of the superstructure

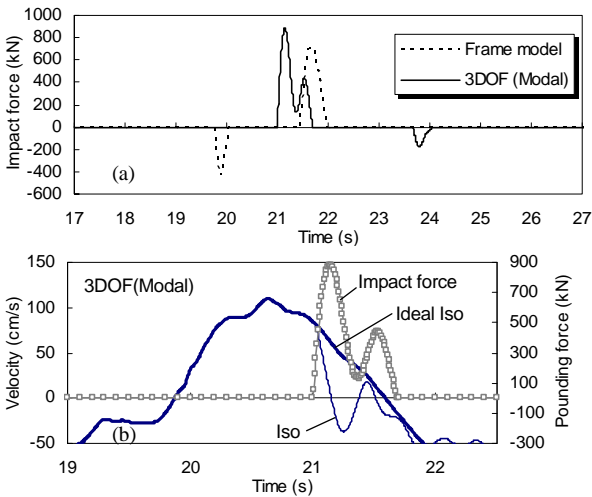


Figure 4 Time history response under CHY101-N input

However, even if the impact velocities are similar, the lumped mass 3DOF models still can not give deformation results comparable with those of the frame model. This is mainly due to lack of continuous elastic component along its height to spread plastic deformations among different stories. To verify, the isolation layer of the frame model is modified so that it collides with the retaining wall only in the positive direction and the retaining wall clearance in the frame model is reduced to 233mm so that the impact velocity can be similar with that of the 3DOF model. As a

result, the impact velocity becomes 86.6cm/s for the frame model. The impact forces of the 3DOF and the modified frame model are compared in Figure 5. The story drift of the modified model is shown by the dotted line in Figure 3. The deformation patterns of the frame model and 3DOF model are totally different although the impact velocities, impact forces are similar. It is notable that deformation is much more distributed among different stories in the frame model.

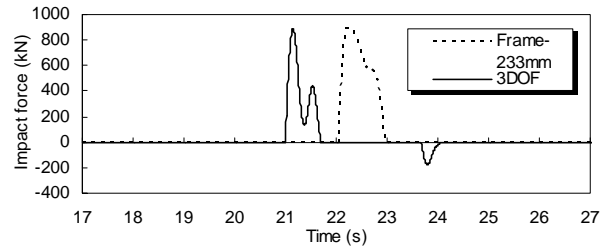


Figure 5 Impact forces under CHY101-N input

Figure 6 compares the story shear changes of the two models. The magnitudes of shear changes of the two models are similar while the rise in story shear travels faster in the 3DOF model than in the frame model.

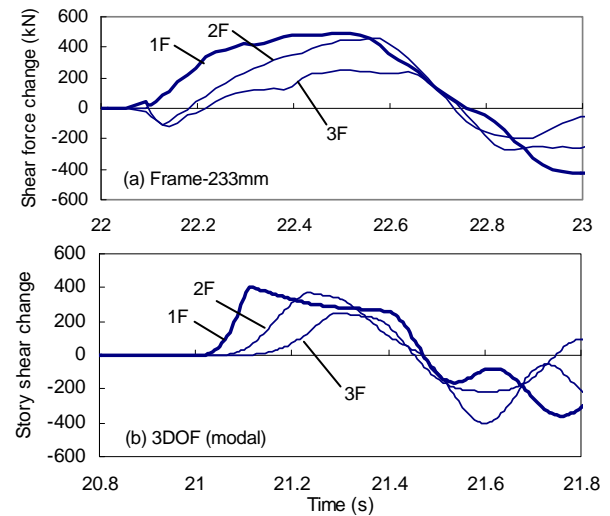


Figure 6 Story shear force during the major collision under CHY101-N input

## 5. Conclusions

The inadequacy of lumped mass MDOF model is demonstrated. It seems especially inappropriate to use such models to estimate the pounding responses of base-isolated buildings. The occurrence of pounding tends to amplify the variance in the predicted responses. And MDOF models tend to concentrate the deformation within the bottom floor and thus yield unreliable deformation pattern.

### Reference

- 1) AIJ. Standard for structural calculation of reinforced concrete structures, 2010.
- 2) Nakanishi, R., et al. Fragility evaluation of base-isolated buildings. Part 1: Seismic response analysis considering bumping against retaining wall. Summaries of technical papers of AIJ annual meeting, B2, 941-942, 2007
- 3) AIJ. Recommendation for loads on buildings, 2004: 66-67.